CrystEngComm

Accepted Manuscript

Experimental and theoretical study of Pb···S and Pb···O σ-hole interactions in the crystal structures of Pb(II) complexes

Juan D. Velásquez[a], Ghodrat Mahmoudi[b*], Ennio Zangrando[c], Atash V. Gurbanov[d,e], Fedor I. Zubkov[f], Yunus Zorlu[g], Ardavan Masoudiasl[b] and Jorge Echeverría[a*]

[a]Departament de Química Inorgànica i Orgànica and Institut de Química Teòrica i Computacional (IQTC-UB), Universitat de Barcelona, Martí i Franquès 1-11, 08028 Barcelona (Spain). E-mail: jorge.echeverria@qi.ub.es

[b] Department of Chemistry, Faculty of Science, University of Maragheh, P.O. Box 55181-83111, Maragheh, Iran. E-mail: mahmoudi_ghodrat@yahoo.co.uk

[c]Department of Chemical and Pharmaceutical Sciences, University of Trieste, Via L. Giorgieri 1, 34127 Trieste, Italy.

[d]Centro de Química Estrutural, Complexo I, Instituto Superior Técnico, Universidade de Lisboa, Av. Rovisco Pais, 1049-001, Lisbon, Portugal,

[e]Department of Chemistry, Baku State University, Z. Khalilov Str. 23, AZ1148, Baku, Azerbaijan

[f]Organic Chemistry Department, RUDN University, Miklukho-Maklaya str. 6, 117198 Moscow, Russian Federation

[g]Department of Chemistry, Gebze Technical University, Gebze, Turkey

Abstract

We report here the synthesis of two new Pb(II) compounds in which the lead center is coordinated by organic ligands via S and O donor atoms. Remarkably, in both compounds the Pb coordination is hemidirectional, which facilitates the approach of extra donors to establish interactions at longer distances. Such interactions are of σ-hole nature between the Pb and O/ S atoms, acting as Lewis acid and bases, respectively. Interestingly, the Pb···S/O distances are closer to the sum of the covalent radii than to the van der Waals ones, which suggests a considerably strong interaction. We have performed a structural analysis of the crystal structures as well as a theoretical analysis based on DFT calculations to gain deeper insight into the origin and features of these σ-hole interactions. Moreover, the nature of the Pb···S/O interactions have been further analysed by means of AIM, MEP and NBO calculations.

Electronic Supplementary Information (ESI) available. CCDC 1935397 and 1935400 contain the supplementary crystallographic data for compounds **1** and **2**.

View Article Online
DOI: 10.1039/C9CE00959K

1. Introduction

Lead, despite its toxicity and the environmental problems associated to it,[1] is a very interesting element that can adopt different coordination geometries when forming compounds.[2] Furthermore, inert pair effect allows the synthesis of many stable Pb(II) complexes. It is known that, in the crystal structures of such compounds, Pb atoms can establish σ-hole interactions with lone pairs of donor atoms.[3] σ-hole interactions occur between an electron-deficient region and an electron-rich species forming an electrostatic attraction as well as a more or less significant electron delocalization from the lone pair into an empty orbital.[4, 5] This dual nature strengthens the interaction and σ-hole bonding is usually used in supramolecular design and crystal design. For instance, σ-hole interactions have been used for the construction of metal Pb(II) organic frameworks (MOFs) by taking advantage of geometrically predictable Pb···O/S/N short contacts.[6-9]

From a topological point of view, the Pb center must be hemidirectionally coordinated for the establishment of σ-hole interactions. A recent CSD survey showed that hemidirectional Pb(II) has a marked tendency to participate in intermolecular short contacts with donor groups that lie between the sum of the corresponding covalent and van der Waals radii.[10] However, and despite their abundance, these σ-hole interactions are not yet fully understood and a better knowledge of them should lead to more simple and accessible ways of exploiting them in solid-state chemistry.

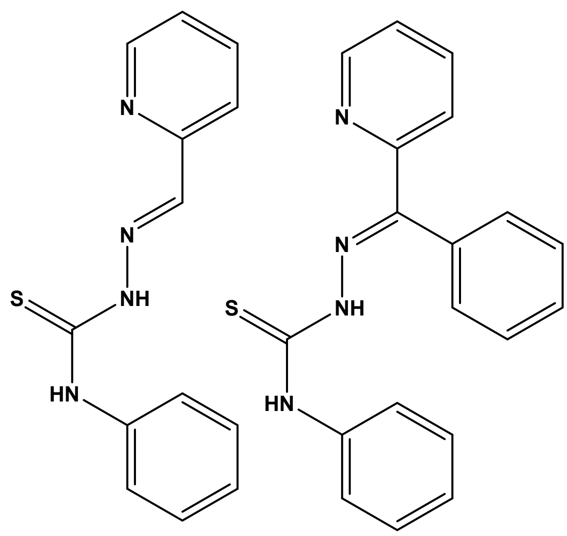

HL[1] **HL[2]**

Scheme 1: Ligands used in this work

In this work, the replacement of O with S atom in coordination sphere of Pb to investigate the effect of tetrel bonding has been studied. For this reason two new Pb(II) complexes of phenyl-thiosemicarbazone based ligands with a anionic coligand (HL^1 and HL^2; see scheme 1) have been

View Article Online
DOI: 10.1039/C9CE00959K

synthesized and characterized by structural, analytical and spectroscopic methods. The ligands coordinate to the Pb(II) metal center in a tridentate fashion via two nitrogen and one sulfur donor atoms either in mono-deprotonated or in neutral forms (scheme 2). Single-crystal X-ray crystallography reveals that the molecular complexes aggregate into larger entities depending on weak interactions. The Pb(II) center is hemidirectionally coordinated and, consequently, it is sterically ideal for establishing σ-hole bonding interactions. Thus, in the crystal structures of both complexes, the Pb participates in short contacts with oxygen or sulfur atoms that can be defined as noncovalent tetrel bonding interactions. We have analysed the interesting supramolecular assemblies observed in the solid state of both complexes by means of DFT calculations and characterized using the Bader's quantum theory of atoms-in-molecules (QTAIM) and Natural Bond Orbitals (NBO) analysis.

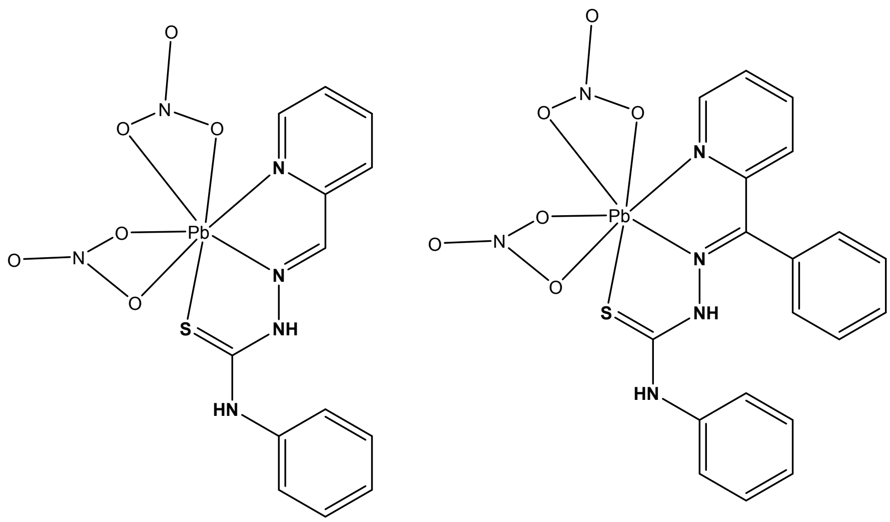

Scheme 2: Complexes **1** and **2** reported in this work

2. Experimental

Due to the insolubility of these compounds in most of the common solvents employed, we failed to crystallize the materials as single crystals in the past. A solution to our inability to grow single-crystals is the use of very interesting and unusual glassware for reaction/crystallization apparatus (branched tube) recently developed by us.[10] The complexes **1** and **2** were synthesized by means of this procedure using the $Pb(NO_3)_2$ salt with HL^1 and HL^2 respectively.

Synthesis of **1**: $Pb(NO_3)_2$ and HL^1 (0.164 g, 0.500 mmol and 0.500 mmol; 0.120) were placed in the main arm of a branched tube. Methanol (15 ml) was carefully added to fill the arms. The tube was sealed and immersed in an oil bath at 60 °C while the branched arm was kept at ambient temperature. After 6 days, crystals of **1** that isolated in the cooler arm were filtered off, washed with acetone and ether, and dried in air.

View Article Online
DOI: 10.1039/C9CE00959K

[Pb(HL[1])(NO_3)$_2$] (**1**) Isolated yield was 72%. Anal. calcd. (found) for $C_{13}H_{12}N_6O_6PbS$; C, 27.32 (27.26); H, 2.12 (2.20); N, 14.71 (14.60)%. IR (cm−1) selected bands: ṽ = CH b (oop): 667 (m) and 779 (m); NOst: 1387 (m); CCst: 1461 (m); C=N st: 1499 and 1585 (m); C=S st (Ligand) 760(m)cm^{-1}.

Synthesis of **2**: $Pb(NO_3)_2$ and HL[2] (0.164 g, 0.500 mmol and 0.500 mmol; 0.166) were used to prepare it. The same procedure as in 1 was followed.

[Pb(HL[2])(NO_3) (**2**) Isolated yield was 51%. Anal. calcd. (found) for $C_{19}H_{15}N_5O_3PbS$; C, 39.04 (39.15); H, 2.59 (2.48); N, 11.98 (11.88)%. IR (cm−1) selected bands: ṽ = CH b (oop): 694 (m) and 774 (m); C=S st (Ligand) 781(m); N-N; 1109(m); NOst: 1380 (m); CCst: 1431 (m); C=N st: 1476 and 1591 (m)cm^{-1}.

Table 1. Crystallographic Data and Details of Refinements for compounds **1-2**

	1	**2**
empirical formula	$C_{13}H_{12}N_6O_6PbS$	$C_{19}H_{15}N_5O_3PbS$
fw	587.54	600.61
Temperature, K	296(2)	296(2)
crystal system	Monoclinic	Monoclinic
space group	$P2_1/c$	$C2/c$
a (Å)	11.9203(7)	37.250(5)
b (Å)	19.9475(11)	5.0731(6)
c (Å)	7.7761(4)	22.594(3)
β (°)	103.949(3)	110.797(14)
V/(Å^3)	1794.48(17)	3991.5(9)
Z	4	8
D_{calcd} (mg/m^3)	2.175	1.999
μ (mm^{-1})	9.563	8.590
F(000)	1112	2288
θ range (°)	2.04-25.01	1.17-27.11
collected reflections	20833	33393
indep reflections	3161	4416
*R*int	0.0407	0.0240
Obs reflections [$I > 2\sigma(I)$]	2858	3820
parameters	250	265
*R*1 [$I > 2\sigma(I)$] [a]	0.0214	0.0287
*wR*2 [$I > 2\sigma(I)$] [a]	0.0504	0.0555
GOF on F^2	1.025	1.042
residuals (e Å^{-3}) [b]	1.323, −1.343	1.165, −1.390

[a] $R1 = \Sigma||Fo|-|Fc|| / \Sigma|Fo|$, $wR2 = [\Sigma w (Fo^2 - Fc^2)^2 / \Sigma w (Fo^2)^2]^{1/2}$
[b] Residuals close to metal atoms.

X-ray crystallography

Suitable single crystals for X-ray analyses of compounds 1-2 were selected and diffraction data were collected with Mo-Kα radiation (λ=0.71073 Å) at 296(2) K on a Bruker APEX II QUAZAR three-circle diffractometer. Data reductions were performed with Bruker APEX2 and SAINT programs.[11] Empirical absorption corrections were applied to all datasets. Both the structures were solved by direct methods and refined by full matrix least-squares procedures using the SHELXTL.[12, 13] All non-hydrogen atoms were refined with anisotropic displacement parameters. The contribution of hydrogen atoms placed at calculated positions (except those attached at N atoms that were located on the Fourier map) was included in the final cycles of refinement. Materials for publication were prepared using Diamond 3.2k.[14, 15] Details of crystallographic data are given in Table 1.

Theoretical methods

Electronic structure calculations were performed with Gaussian09[16] at the M06-2X/def2-TZVP level. This method has shown very good performance for the study of noncovalent interactions.[17, 18] Crystallographic geometries were used with no further optimization. Interaction energies were corrected for the BSSE by means of the Counterpoise method.[19] QTAIM[20] analyses of the topology of the electron density were carried out with the AIMAll software[21] at the same level of theory. NCI analysis was done with NCIPLOT.[22, 23] Natural Bond Orbital analysis was done with the NBO3.1 program[24] as implemented in Gaussian09. Molecular electrostatic potential (MEP) maps were built on the van der Waals surfaces ($s = 0.002$ e Å^{-3}) with GaussView.[25] We used the set of covalent and van der Waals radii proposed by Alvarez.[26, 27]

3. Results and discussion

Compound **1** crystallizes in monoclinic space group $P2_1/c$ and its crystallographic independent unit is shown in Figure 1, while Table 2 reports a selection of coordination bond lengths. The Pb(II) atom is μ_3-chelated by ligand HL^1 through the *S,N,N* donors and covalently linked to two nitrate anions. The Pb-N/O bond distances are within the range 2.512(4)-2.870(4) Å, the Pb-S bond length is of 2.8199(14) Å. The phenyl ring forms a dihedral angle of 41.06° with the chelating part, the atoms of which are almost coplanar. The bond distances of the moiety N1/C7/N2/N3/C8 are of 1.335(5), 1.352(5), 1.364(5) and 1.274(5) Å, indicating an electron delocalization inside the fragment. The $[Pb(HL1)(NO_3)_2]$ units are connected by double pairs of H-bonds (Figure 2) realized between the NH groups and nitrate oxygen of a symmetry related complex (N…O distances of 2.891(5) and 2.831(5) Å, Table 3). In the crystal packing each Pb atom shows additional Pb-O3 tetrel bonds, of 2.934(4) Å, so that a 2D undulated layer is formed parallel to the *bc* plane, having a (6,3) net topology (Figure 3). No significant π-π stacking among py and phenyl rings is detected in the packing.

View Article Online
DOI: 10.1039/C9CE00959K

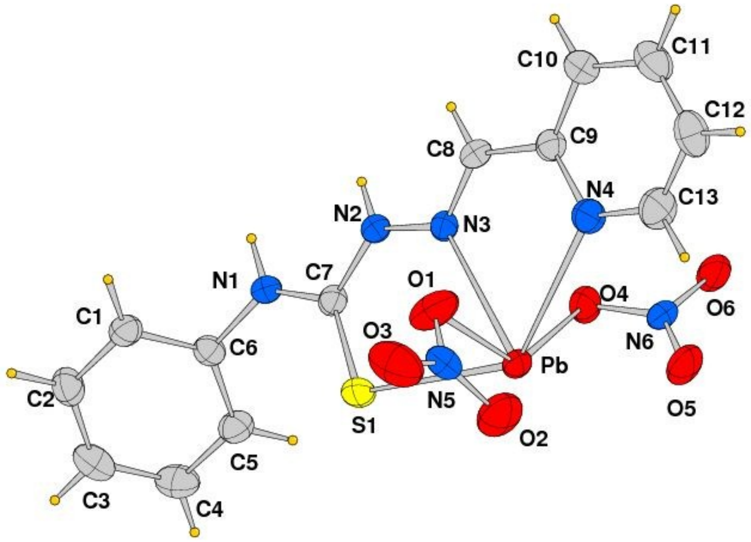

Figure 1. ORTEP drawing (40% probability ellipsoids) of the asymmetric unit of **1.**

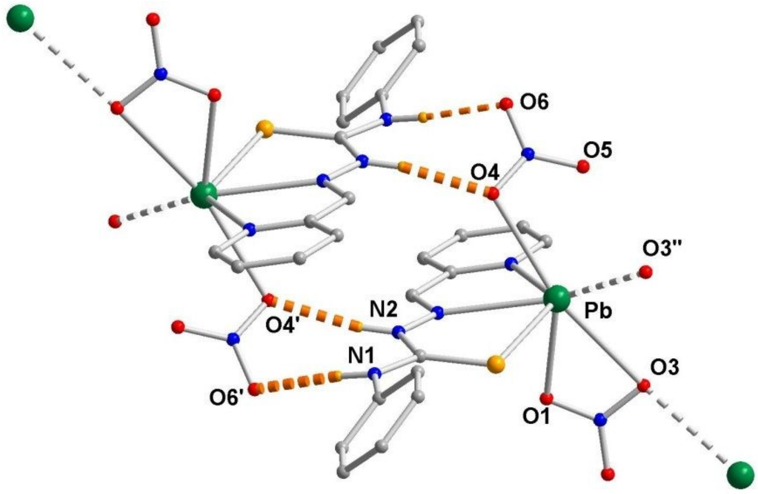

Figure 2. The double pairs of NH…O hydrogen bonds connecting two [Pb(HL1)$(NO_3)_2$] complexes (atom N1' and N2' at 1-x,1-y,1-z; O3'' at x, 1/2-y, 1/2+z).

View Article Online
DOI: 10.1039/C9CE00959K

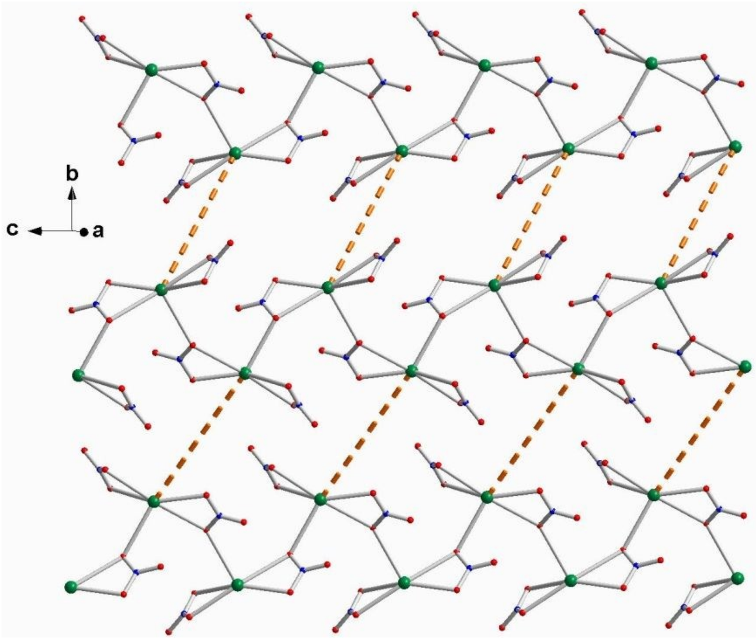

Figure 3. A perspective view of the 2D layer in the crystal packing. The chelating ligands are not shown and the double pairs of H-bonds are replaced by dotted lines for sake of clarity.

Table 2. Selected bond lengths (Å) and angles (°) for complexes **1** and **2**.

1		**2**	
Pb-S(1)	2.8199(14)	Pb-S(1)	2.7680(11)
Pb-N(3)	2.625(3)	Pb-N(3)	2.535(4)
Pb-N(4)	2.684(4)	Pb-N(4)	2.566(4)
Pb-O(1)	2.512(4)	Pb-O(1)	2.509(3)
Pb-O(2)	2.870(4)	Pb-O(2)	2.854(4)
Pb-O(4)	2.693(3)	Pb-S(1')	3.2535(11)
Pb-O(5)	2.926(4)	Pb-S(1")	3.3233(14)
Pb-O(3')	2.934(4)	-	

Table 3. H-bond geometry (Å/deg) for complexes **1** and **2**.

D-H	d(D-H)	d(H..A)	<DHA	d(D..A)	A	Symmetry code
Complex 1						

View Article Online
DOI: 10.1039/C9CE00959K

N(1)-H(1n)	0.87(3)	1.97(3)	175(4)	2.831(5)	O(6)	1-x,1-y,1-z
N(2)-H(2n)	0.89(3)	2.03(3)	165(4)	2.891(5)	O(4)	1-x,1-y,1-z
Complex 2						
N(1)-H(1n)	0.86(4)	2.29(4)	175(4)	3.147(5)	O(2)	1/2-x,5/2-y,1-z

The structural unit of compound **2** [Pb(L2)(NO_3)], which crystallizes in monoclinic space group C2/c, comprises a lead(II) atom chelated by the tridentate deprotonated HL^2 ligand and one nitrate anion (Fig. 4). Here the coordination bond distances Pb-N3, Pb-N4 and Pb-S1 are of 2.535(4), 2.566(4) and 2.7680(11) Å, respectively, significantly shorter by about 0.1 Å with respect to those measured in **1** (Table 1), while Pb-O1 and Pb-O2 bonds are comparable in length to those of the N5 nitrate anion of **1**. The values of bond distances inside the ligand skeleton N1/C7/N2/N3/C8 follow a trend similar to that found in **1** (1.353(5), 1.299(5), 1.378(5), and 1.290(5) Å), indicating an extended electron delocalization. It is worth of note that differently from what detected in **1** the phenyl group and sulfur atom are here positioned trans to the C1-N7 bond. Two [Pb(L2)(NO_3)] fragments are bound through weak N1-H…O2 hydrogen bonds (N…O = 3.147(5) Å, N-H…O = 175(4)°) to form a dimer (Figure 5, Table 2). From a topological point of view, the complexes are connected by Pb-S tetrel bonds of 3.2535(11) and 3.3233(14) Å (beside the above described coordination Pb-S bond of 2.7680(11) Å) to form a double -$[Pb(L2)]_n$- polymer of a stair-like fashion developed along axis *b* (Figure 6). Inside the chain the shorter intermetallic distance is 4.446 Å. The described crystal packing does not show any significant π-π stacking. Coordination bond distances reported here agree with those measured in other previous similar lead structures.[7, 9]

View Article Online
DOI: 10.1039/C9CE00959K

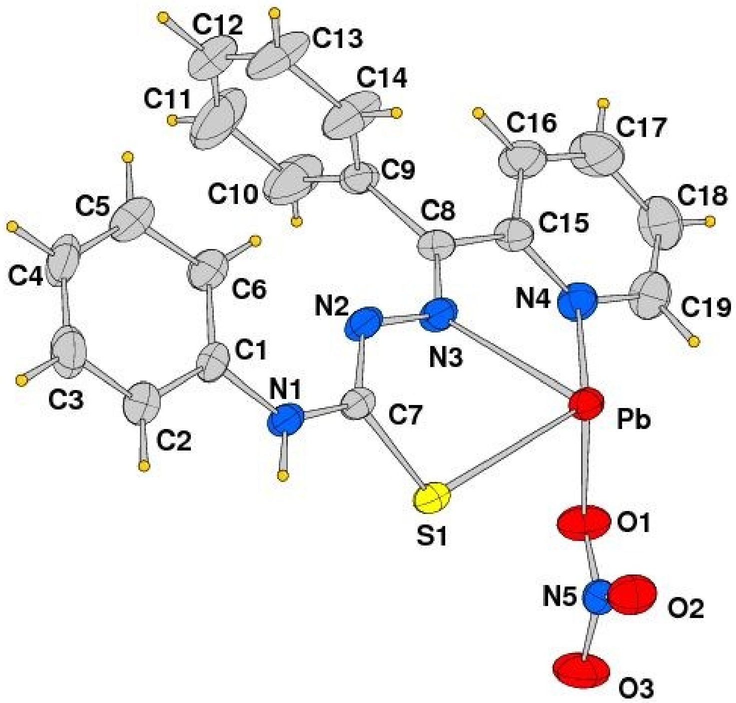

Figure 4. ORTEP drawing (40% probability ellipsoids) of the asymmetric unit of **2**.

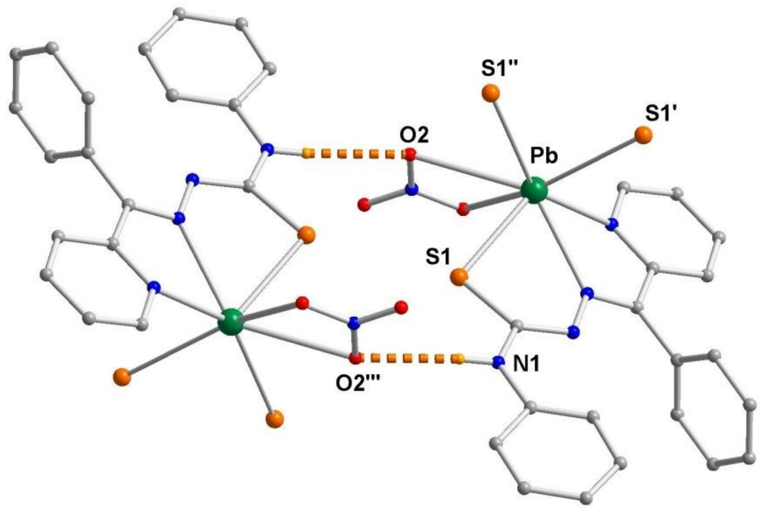

Figure 5. Centrosymmetric dimer formed by the N1-H…O2 hydrogen bonds (symmetry codes: S1' at x, -1+y, z; S1" at 1/2-x, 3/2-y, 1-z; O2''' at 1/2-x, 5/2-y, 1-z).

View Article Online
DOI: 10.1039/C9CE00959K

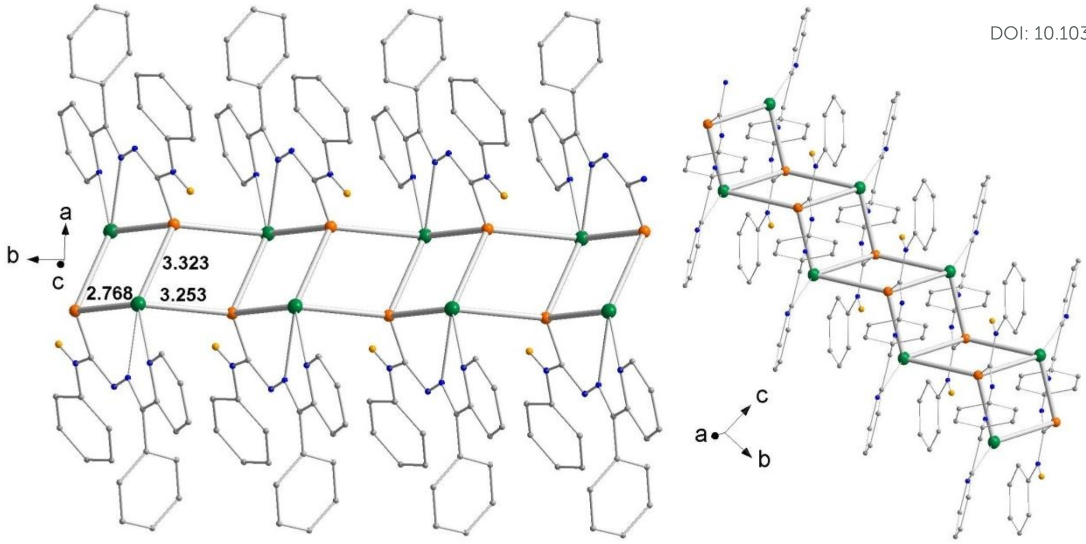

Figure 6. Polymeric structure of complex **2** formed by Pb-S bonding interactions (values in Å).

We have next performed a theoretical analysis of the two species **1** and **2** in their crystal structures to gain further insight into the interactions that hold them together. It is known that atoms of group 14 can engage in intermolecular σ-hole interactions with donor species to form what has been termed a tetrel bond.[28] In **1**, as mentioned above, besides the four H-N···H hydrogen bonds connecting each pair of molecules, the Pb atoms show intermolecular short contacts to the oxygen atoms of the NO_3 chelating ligands (Pb···O = 2.934 and 3.25 Å, see Fig. 7a). We will focus then in these particular interactions involving the Pb centers. The topology of the electron density has been analysed by means of the Quantum Theory of Atoms in Molecules (QTAIM). We have found bond paths between the Pb and the two donor O atoms as shown in Figure 7b confirming the tetrel interaction. The values of the electron density at the associated bond critical points are 0.0175 and 0.0120 au for BCP1 and BCP2, respectively, in good agreement with previous reports for similar interactions.[6, 8] The AIM results also show C-H···π interactions and CH···S hydrogen bonds between the two molecules as characterized by the corresponding bond paths (Figure 7b). The calculated interaction energy associated to the latter dimer is -10.42 kcal/mol (see Theoretical methods for details).

View Article Online
DOI: 10.1039/C9CE00959K

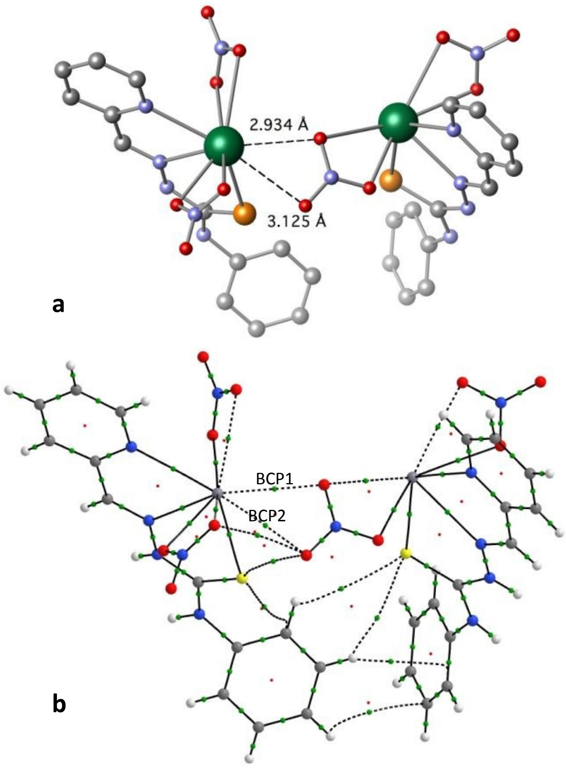

Figure 7. (**a**) Short Pb···O contacts in the crystal structure of **1**. (**b**) QTAIM graph of the interactions found in **1** showing the BCPs as green points.

Next, we focus on the crystal structure of compound **2**. As shown in Figure 6, the molecules are arranged in such a way that they form a 1D chain connected by Pb···S interactions (3.253 and 3.323 Å in crystallographic directions b and a, respectively). The interaction energy of the dimer displaying two intermolecular Pb···S contacts at 3.323 Å is -15.31 kcal/mol (Figure 8a). On the other hand, in the *b* crystallographic direction, we have calculated an interaction energy of -15.47 kcal/mol, for the dimer associated with a Pb···S contact at 3.253 Å and a Pb···O interaction at 3.129 Å (Figure 8b). In order to estimate the strength of solely the Pb···S interaction, we have modified the geometry by orientating the interacting NO_3 group towards the outer part of the molecule, avoiding in this way any Pb···O short contact (the Pb···O distance is now 6.56 Å, see Figure S1 in the ESI). The calculated interaction energy is -10.83 kcal/mol, which also allows us to estimate the strength of the Pb···O short contact (≈ 4.50 kcal/mol). The QTAIM analysis of the dimer of Figure 8a clearly shows that Pb···S tetrel interactions are the only ones holding the two molecules together (see Figure 8c). The value of the electron density at both BCP3 and BCP4 is 0.0163 au and, more interestingly, the value of the delocalization index DI(Pb,S) at the same BCPs is considerably large (0.1764 au), indicating some degree of charge transfer between the two atoms. The picture of the dimer with a a Pb···S contact at 3.253 Å is more complex since more interactions are present in the AIM graph (see Figure 8d).

View Article Online
DOI: 10.1039/C9CE00959K

Besides the Pb···S and Pb···O contacts, a plethora of noncolavent interactions (π/π, C-H···π, C-H···O) are determined by bond paths and BCPs. BCP6, which corresponds to the shortest Pb···S contact, presents the highest value of the electron density among all characterized here (0.0177 au). The values of several properties for all the BCPs analysed here can be found in the Supporting Information (Table S1).

Since many BCPs and BPs are found in the QTAIM analysis depicted in Fig. 8d, we have performed a NCI analysis[22] of the dimer to try to clarify the different interactions present. The Pb···S and Pb···O interactions are clearly present (Figure 9). Moreover, secondary interactions between the aromatic ligands are of the type π/π and CH···π as already observed in the QTAIM graphs of Fig. 8d.

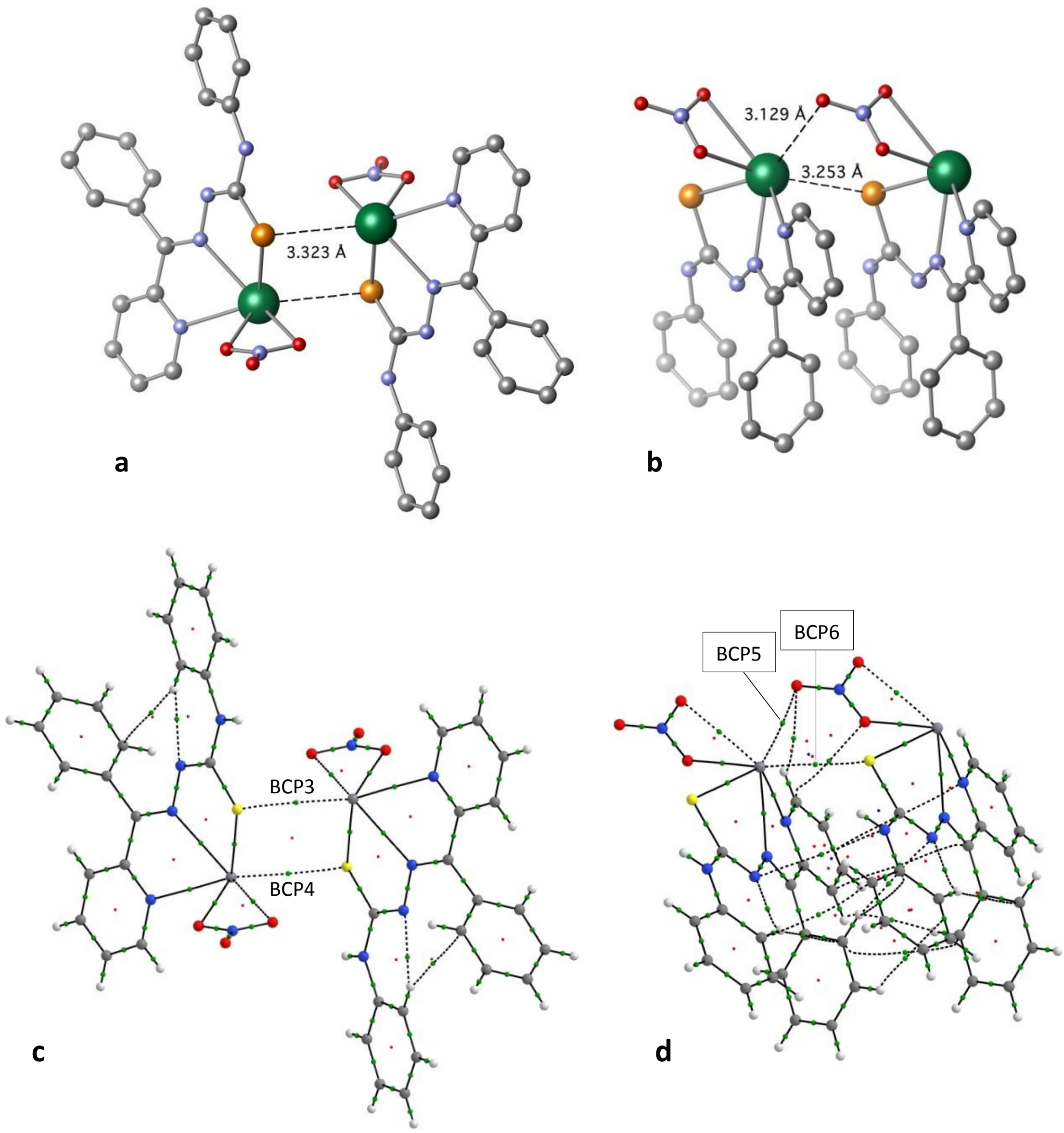

Figure 8. The two dimers analysed in the crystal structure of **2** in the (**a**) *a* and (**b**) *b* crystallographic directions, and their corresponding QTAIM graphs (**c** and **d**).

View Article Online
DOI: 10.1039/C9CE00959K

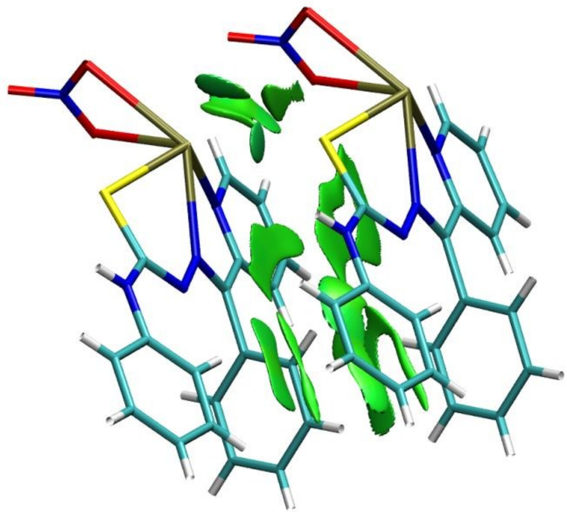

Figure 9. NCI plot of the dimer **2** in the *b* crystallographic direction. Green areas represent regions of weak non-covalent interactions.

With significant electrostatic contribution to the interaction energy, σ-hole interactions can also be characterized by mapping the molecular electrostatic potential (MEP) of the molecules involved since electron rich regions with negative values of MEP are prone to interact with electron deficient regions of positive MEP.[29-32] In the MEP map of complex **2**, the two areas are clearly differentiated (Figure 10): The sulphur and the oxygen atoms of the nitrato ligand with negative MEP and, on the other hand, the exposed region of the Pb atom with positive MEP. This is consistent with the interaction pattern present in the crystal structure of **2**, where these two regions interact with each other to establish tetrel bonds.

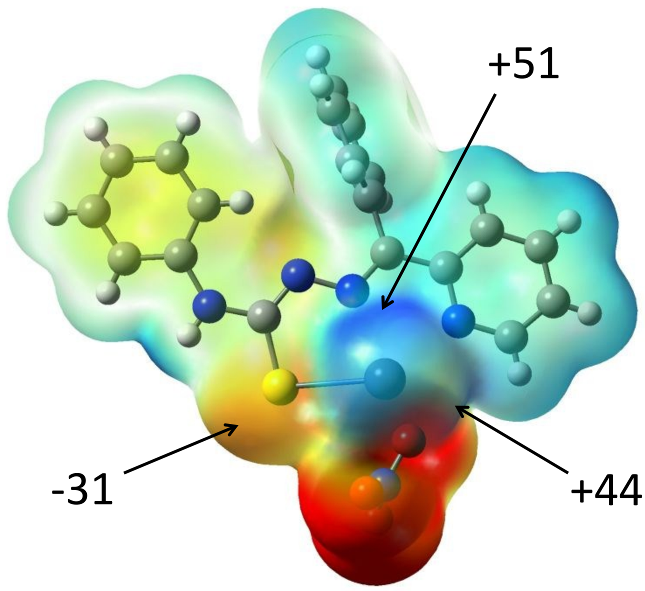

View Article Online
DOI: 10.1039/C9CE00959K

Figure 10. MEP map of compound **2** plotted on the 0.002 e Å^{-3} isosurface. Blue represents more positive and red more negative electrostatic potential. Energies are given in kcal/mol.

Since tetrel bonding also has a non-negligible orbital character, which has also been suggested by the calculated delocalization indexes in our AIM study above, we have performed an NBO analysis of the two short Pb···S contacts present in the crystal structure of **2**. In both cases we observe an interaction between the S lone pairs and a Pb empty orbital. For the Pb···S contact at 3.323 Å such interaction accounts for 14.89 kcal/mol whereas in the contact at 3.253 Å the associated NBO energy is 17.59 kcal/mol. This is in good agreement with the observed interatomic distances since a shorter contact should increase the orbital overlap. The electron delocalization is confirmed by looking at the occupancies of the orbitals involved in the interaction. For instance, for the contact at 3.253 Å, the S lone pair orbitals contain 1.949 and 1.818 electrons, respectively, while the occupancy of the acceptor orbital at the Pb is 0.1897.

4. Conclusions

In this report, we have synthesized two new Pb(II) complexes with phenyl-thiosemicarbazone Schiff base ligands. In their crystal structures, these complexes show hemidirected coordination modes that allow them to establish σ-hole interactions with lone pairs from oxygen and sulfur atoms. The Pb···S/O contact distances are longer than the sum of the covalent radii and shorter than the sum of the van der Waals radii. The strength of the interactions have been calibrated by means of DFT calculations and their nature studied via AIM, MEP and NBO analyses. The σ-holes interactions studied here show associated interaction energies between 10 and 15 kcal/mol. Moreover, we have observed that both electrostatic and orbital interactions contribute to the total attraction between Pb and S/O. On one hand, electrostatic attraction can be rationalized in terms of the electrostatic potential of the interacting regions and, on the other hand, NBO analysis has revealed a charge transfer from O/S lone pairs to an empty orbital of Pb. These results are expected to be useful for the development of new Pb-containing MOFs in which supramolecular assembly is dominated by σ-hole interactions.

Conflict of interest

There are no conflicts to declare.

Acknowledgements

We are grateful to the University of Maragheh and Iran Science Elites Federation (ISEF) for the financial support of this research. The publication was prepared with the support of the RUDN

View Article Online
DOI: 10.1039/C9CE00959K

University Program 5-100. A.V.G acknowledges the FCT and Instituto Superior Técnico (DL 57/2016 and L 57/ 2017 Program, Contract no: IST-ID/110/2018). J.E. thanks the Spanish MICINN (RYC-2017-22853) and MINECO (MDM-2017-0767) for funding. J.D.V. acknowledges the Universitat de Barcelona for a predoctoral APIF grant.

References

1. D. A. Gidlow, *Occupational Medicine-Oxford*, 2015, **65**, 348-356.
2. J. Parr, *Polyhedron*, 1997, **16**, 551-566.
3. A. Bauzá, S. K. Seth and A. Frontera, *Coord. Chem. Rev.*, 2019, **384**, 107-125.
4. J. S. Murray, P. Lane and P. Politzer, *J. Mol. Model.*, 2009, **15**, 723-729.
5. J. S. Murray, P. Lane, T. Clark, K. E. Riley and P. Politzer, *J. Mol. Model.*, 2012, **18**, 541-548.
6. S. K. Seth, A. Bauzá, G. Mahmoudi, V. Stilinović, E. López-Torres, G. Zaragoza, A. D. Keramidas and A. Frontera, *CrystEngComm*, 2018, **20**, 5033-5044.
7. G. Mahmoudi, E. Zangrando, M. P. Mitoraj, A. V. Gurbanov, F. I. Zubkov, M. Moosavifar, I. A. Konyaeva, A. M. Kirillov and D. A. Safin, *New J. Chem.*, 2018, **42**, 4959-4971.
8. G. Mahmoudi, S. K. Seth, A. Bauzá, F. I. Zubkov, A. V. Gurbanov, J. White, V. Stilinović, T. Doert and A. Frontera, *CrystEngComm*, 2018, **20**, 2812-2821.
9. G. Mahmoudi, A. Bauzá, A. Frontera, P. Garczarek, V. Stilinović, A. M. Kirillov, A. Kennedy and C. Ruiz-Pérez, *CrystEngComm*, 2016, **18**, 5375-5385.
10. M. Servati Gargari, V. Stilinović, A. Bauzá, A. Frontera, P. McArdle, D. Van Derveer, S. W. Ng and G. Mahmoudi, *Chem. Eur. J.*, 2015, **21**, 17951-17958.
11. Bruker (2012). APEX2 and SAINT programs. Bruker AXS Inc., Madison, Wisconsin, USA.
12. SHELXS-97, Program for crystal structure solution, G.M. Sheldrick - 1997- University of Göttingen, Germany.
13. G. M. Sheldrick, *Acta Crystallogr.*, 2008, 112.
14. K. Brandenburg, (1999). DIAMOND. Crystal Impact GbR, Bonn, Germany program and WINGX package (Ver 2013.3). .
15. L. J. Farugia, *Appl. Cryst.*, 2012, **45**, 849-854.
16. Gaussian 09, Revision D.01, Frisch, M. J.; Trucks, G. W.; Schlegel, H. B.; Scuseria, G. E.; Robb, M. A.; Cheeseman, J. R.; Scalmani, G.; Barone, V.; Mennucci, B.; Petersson, G. A.; Nakatsuji, H.; Caricato, M.; Li, X.; Hratchian, H. P.; Izmaylov, A. F.; Bloino, J.; Zheng, G.; Sonnenberg, J. L.; Hada, M.; Ehara, M.; Toyota, K.; Fukuda, R.; Hasegawa, J.; Ishida, M.; Nakajima, T.; Honda, Y.; Kitao, O.; Nakai, H.; Vreven, T.; Montgomery, J. A., Jr.; Peralta, J. E.; Ogliaro, F.; Bearpark, M.; Heyd, J. J.; Brothers, E.; Kudin, K. N.; Staroverov, V. N.; Kobayashi, R.; Normand, J.; Raghavachari, K.; Rendell, A.; Burant, J. C.; Iyengar, S. S.; Tomasi, J.; Cossi, M.; Rega, N.; Millam, J. M.; Klene, M.; Knox, J. E.; Cross, J. B.; Bakken, V.; Adamo, C.; Jaramillo, J.; Gomperts, R.; Stratmann, R. E.; Yazyev, O.; Austin, A. J.; Cammi, R.; Pomelli, C.; Ochterski, J. W.; Martin, R. L.; Morokuma, K.; Zakrzewski, V. G.; Voth, G. A.; Salvador, P.; Dannenberg, J. J.; Dapprich, S.; Daniels, A. D.; Farkas, Ö.; Foresman, J. B.; Ortiz, J. V.; Cioslowski, J.; Fox, D. J. Gaussian, Inc., Wallingford CT, 2009.
17. S. Kozuch and J. M. L. Martin, *J. Chem. Theory Comput.*, 2013, **9**, 1918-1931.
18. A. Bauzá, I. Alkorta, A. Frontera and J. Elguero, *J. Chem. Theory Comput.*, 2013, **9**, 5201-5210.
19. S. F. Boys and F. Bernardi, *Mol. Phys.*, 1970, **19**, 553-566.
20. R. F. W. Bader, *Atoms in Molecules: A Quantum Theory*, Clarendon Press, Oxford, 1990.

21. AIMAll (Version 16.08.17), Todd A. Keith, TK Gristmill Software, Overland Park KS, USA, 2016 (aim.tkgristmill.com).
22. E. R. Johnson, S. Keinan, P. Mori-Sánchez, J. Contreras-García, A. J. Cohen and W. Yang, *J. Am. Chem. Soc.*, 2010, **132**, 6498-6506.
23. J. Contreras-García, E. R. Johnson, S. Keinan, R. Chaudret, J.-P. Piquemal, D. N. Beratan and W. Yang, *J. Chem. Theory Comput.*, 2011, **7**, 625-632.
24. NBO Version 3.1, E. D. Glendening, A. E. Reed, J. E. Carpenter, and F. Weinhold.
25. GaussView, version 5, R. Dennington, T. Keith and J. Millam, Semichem Inc., Shawnee Mission, KS, 2009.
26. B. Cordero, V. Gómez, A. E. Platero-Prats, M. Revès, J. Echeverría, E. Cremades, F. Barragán and S. Alvarez, *Dalton Trans.*, 2008, 2832-2838.
27. S. Alvarez, *Dalton Trans.*, 2013, **42**, 8617-8636.
28. A. Bauzá, T. J. Mooibroek and A. Frontera, *Angew. Chem. Int. Ed.*, 2013, **52**, 12317-12321.
29. J. Echeverría, *Phys. Chem. Chem. Phys.*, 2017, **19**, 32663-32669.
30. J. Echeverría, *CrystEngComm*, 2017, **19**, 6289-6296.
31. J. Echeverría, *ChemPhysChem*, 2017, **18**, 2864-2872.
32. J. Echeverría, *Cryst. Growth Des.*, 2018, **18**, 506-512.

View Article Online
DOI: 10.1039/C9CE00959K

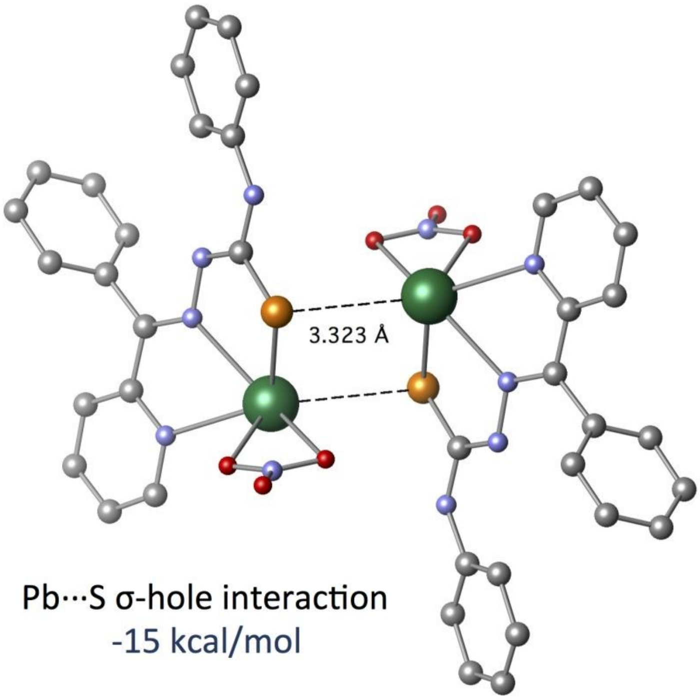

The crystal structures of two novel Pb(II) hemidirected compounds present considerably strong Pb···S σ-hole bonding as the main intermolecular interactions.